

An X-ray Census of Active Galactic Nuclei in the Virgo and Fornax Clusters of Galaxies with SRG/eROSITA

MEICUN HOU ¹, ZHENSONG HU ^{2,3} AND ZHIYUAN LI ^{2,3}

¹*Kavli Institute for Astronomy and Astrophysics, Peking University, Beijing 100871, China*

²*School of Astronomy and Space Science, Nanjing University, Nanjing 210023, China*

³*Key Laboratory of Modern Astronomy and Astrophysics (Nanjing University), Ministry of Education, Nanjing 210023, China*

ABSTRACT

We present a uniform and sensitive X-ray census of active galactic nuclei (AGNs) in the two nearest galaxy clusters, Virgo and Fornax, utilizing the newly released X-ray source catalogs from the first all-sky scan of SRG/eROSITA. A total of 50 and 10 X-ray sources are found positionally coincident with the nuclei of member galaxies in Virgo and Fornax, respectively, down to a 0.2–2.3 keV luminosity of $\sim 10^{39}$ erg s^{−1} and reaching out to a projected distance well beyond the virial radius of both clusters. The majority of the nuclear X-ray sources are newly identified. There is weak evidence that the nuclear X-ray sources are preferentially found in late-type hosts. Several hosts are dwarf galaxies with a stellar mass below $\sim 10^9$ M_⊙. We find that contamination by non-nuclear X-ray emission can be neglected in most cases, indicating the dominance of a genuine AGN. In the meantime, no nuclear X-ray source exhibits a luminosity higher than a few times 10^{41} erg s^{−1}, which might be owing to a steep intrinsic luminosity function. The X-ray AGN occupation rate is only $\sim 3\%$ in both clusters, apparently much lower than that in field galaxies inferred from previous X-ray studies. Both aspects suggest that the cluster environment effectively suppresses AGN activity. The findings of this census have important implications on the interplay between galaxies and their central massive black holes in cluster environments.

Keywords: Galaxy clusters(584) — Virgo Cluster(1772) — X-ray astronomy(1810) — X-ray active galactic nuclei (2035)

1. INTRODUCTION

Active galactic nuclei (AGNs), the manifestation of accreting super-massive black holes (SMBHs) at the center of most galaxies (Padovani et al. 2017), play an indispensable and increasingly crucial role in our understanding of the formation and growth of these exotic objects, as well as their interplay and co-evolution with the host galaxies (Fabian 2012; Kormendy & Ho 2013).

From the very beginning (Schmidt 1963), AGN studies, in particular the demography of AGNs, have benefitted from two lines of research: towards greater distances and towards larger samples. The recently launched James Webb Space Telescope with its unprece-

dented sensitivity in the infrared window is now unveiling some of the first-generation AGNs at the early universe (Goulding et al. 2023). On the other hand, wide-field, even all-sky, surveys of AGNs in the low-redshift universe continue to offer new insights and surprises by revealing a vastly large number of AGNs otherwise lurking at the center of normal and dwarf galaxies. Most of these low-redshift AGNs turn out to have low luminosities (Ho 2008), which trace weakly accreting SMBHs fed by a radiatively inefficient, hot accretion flow (Yuan & Narayan 2014). Growing attention has been paid by recent observational and theoretical studies about the importance of such weakly accreting SMBHs in our understanding of the SMBH-host galaxy co-evolution (e.g. Weinberger et al. 2017; Yoon et al. 2019; Shi et al. 2021). Alternatively, a small fraction of these low-luminosity AGNs could be smaller black holes accreting at a rate closer to the Eddington limit. Such dwarf MBHs or intermediate-mass black holes (IMBHs) are the long-

houmc@pku.edu.cn

huzhensong@smail.nju.edu.cn

lizy@nju.edu.cn

sought population that bridges the stellar-mass black holes and SMBHs (Greene et al. 2020).

X-rays, which trace the hot plasma in and around the accretion flow onto the SMBH, provide arguably the most direct evidence for AGNs. This has been demonstrated, in particular, by the *Chandra* Deep Field surveys of distant AGNs up to a redshift $z \gtrsim 6$ (Giaccconi et al. 2002; Luo et al. 2017; Xue 2017). The superb sensitivity and angular resolution of *Chandra* has also enabled routine detections of nuclear X-ray sources down to the Eddington limit of solar-mass objects ($\sim 10^{38}$ erg s $^{-1}$) in nearby galaxies (e.g. Gallo et al. 2008; She et al. 2017), enabling the study of specific AGNs as well as AGN demography across diverse galactic environments.

The environment is believed to play a crucial role in galaxy evolution. In particular, in galaxy clusters, where individual galaxies travel at a typical velocity of $\sim 10^3$ km s $^{-1}$ within the hot intra-cluster medium (ICM) and frequently interact with other galaxies, environmental effects such as ram pressure stripping (Boselli et al. 2022) and tidal interaction continue to shape the member galaxies and their interstellar medium (ISM). It is generally expected that the long-term outcome of such effects would be to reduce the amount of the ISM, quench star formation and suppress the SMBH accretion.

Observational evidence for starving SMBHs in the nearest galaxy cluster, Virgo, was obtained by the AGN Multi-wavelength Survey of Early-Type Galaxies in the Virgo Cluster (AMUSE-Virgo; Gallo et al. 2008, 2010), which probed nuclear X-ray sources in 100 early-type galaxies (ETGs; including elliptical, lenticular, and dwarf elliptical/lenticular), finding an occupation fraction of 24% – 34% down to an X-ray luminosity of few times 10^{38} erg s $^{-1}$. A similar occupation fraction of X-ray AGNs is found for a sample of ETGs in the second nearest cluster, Fornax (Lee et al. 2019), and the third nearest cluster, Antlia (Hu et al. 2023), down to a comparable detection limit. On the other hand, among the AMUSE-Field sample of 103 nearby field and group ETGs, collectively designed as a ‘field’ comparison for AMUSE-Virgo, Miller et al. (2012) reported a higher X-ray AGN occupation fraction of $45\% \pm 7\%$ and a higher nuclear X-ray luminosity at a given black hole mass than the Virgo ETG sample. Soria et al. (2022) and Graham et al. (2021) have gathered a sample of 75 late-type galaxies (LTGs, including normal disks and dwarf irregulars) in Virgo, finding more than half hosting a nuclear X-ray source, again down to a detection limit of few times 10^{38} erg s $^{-1}$.

These studies, all based on sensitive *Chandra* observations, provide an important insight on how the AGN activity may be related to the intrinsic properties of host galaxies continuously being modified by the environmental effects. Nevertheless, the sample galaxies covered by these programs are just a small fraction of the identified member galaxies in the respective clusters, and perhaps more unsatisfactorily, are biased to large galaxies and/or galaxies in the cluster core due to the design of the individual programs.

Thanks to the advent of the SRG/eROSITA all-sky survey (Sunyaev et al. 2021), a uniform and sensitive soft-X-ray census of AGNs in the two nearest galaxy clusters is within reach for the first time. Although the point source sensitivity of eROSITA is no better than that of *Chandra* due to its moderate point-spread function (with a half-energy width [HEW] $\sim 30''$; Merloni et al. 2024), a sensitivity limit down to $\sim 10^{39}$ erg s $^{-1}$ is readily achievable, sufficient to detect low-luminosity AGNs expected to be prevalent in these two clusters. We take up such a task in this work, utilizing the freshly released eROSITA data from its first all-sky scan (eRASS1).

The remainder of this paper is structured as follows. The catalogues of Virgo and Fornax galaxies are described in Section 2. The identification of nuclear X-ray sources from eRASS1 are described in Section 3. Statistical analyses of the nuclear X-ray sources are presented in Section 4, focusing on the X-ray AGN occupation fraction as a function of various galaxy properties. A brief summary and some immediate implications of our findings are addressed in Section 5.

2. MEMBER GALAXIES OF VIRGO AND FORNAX

To identify X-ray AGNs in the two clusters, we employ the Extended Virgo Cluster Catalog (EVCC; Kim et al. 2014) and the Fornax Cluster Catalog (FCC; Ferguson 1989), which provide the most up-to-date, uniformly classified member galaxies of the respective clusters.

The EVCC contains a total of 1589 spectroscopically identified galaxies, based primarily on the Sloan Digital Sky Survey (SDSS) and supplemented by spectroscopic data from the literature. The footprint of EVCC is more than 5 times that of the photography-based Virgo Cluster Catalog (Binggeli et al. 1985) and reaches out to a projected distance 3.5 times the virial radius of Virgo ($R_{200} \approx 1.0$ Mpc; Simionescu et al. 2017). As detailed in Kim et al. (2014), within this footprint, nearly 100% of the SDSS photometric galaxies with a *r*-band magnitude $r \lesssim 14$ mag have a spectroscopic redshift, and the 50% completeness level for galaxies having a radial

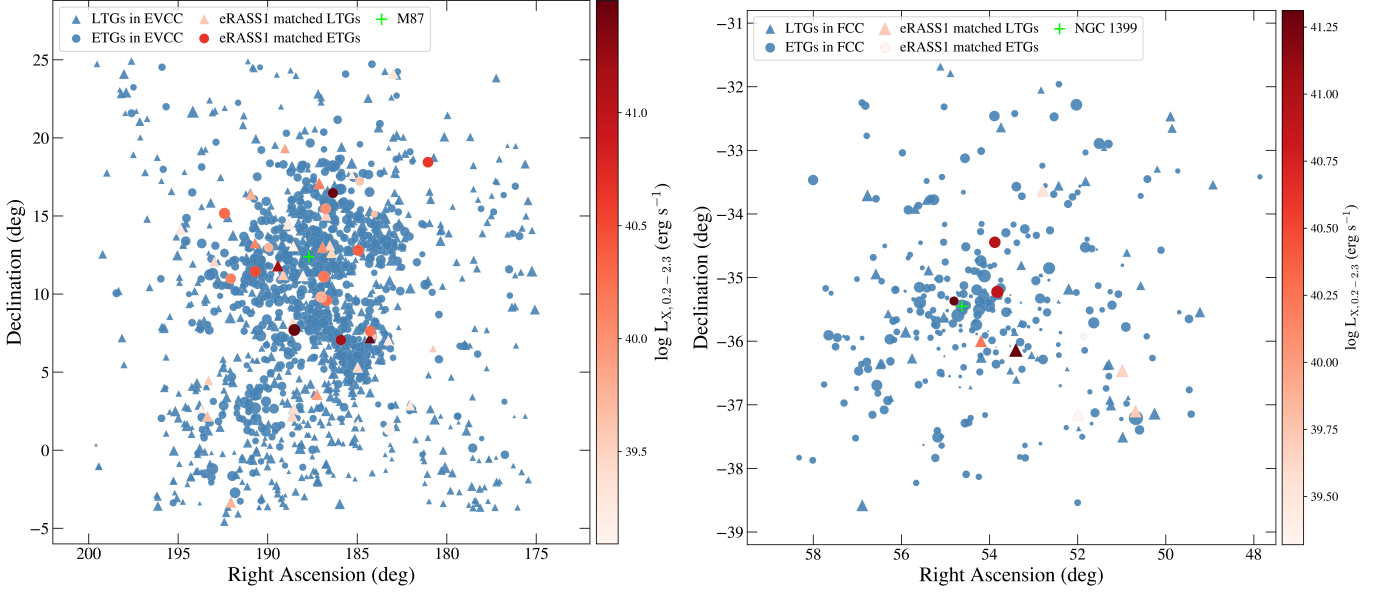


Figure 1. The sky distribution of member galaxies in Virgo (*left*) and Fornax (*right*). Member galaxies in the Extended Virgo Cluster Catalog and Fornax Cluster Catalog are indicated by blue symbols. The nuclear X-ray sources detected by eRASS1 are marked by red symbols color-coded by the 0.2–2.3 keV luminosity. ETGs and LTGs are represented by circles and triangles. The size of each symbol is scaled with stellar mass (approximated by B_T mag for the Fornax galaxies).

velocity $< 3000 \text{ km s}^{-1}$ (i.e., the criterion for a Virgo member) is at $r \sim 16.5$ mag. The latter value translates to an absolute magnitude of $M_r \approx -14.1$ for the nominal distance of Virgo (16.5 Mpc; Mei et al. 2007), roughly corresponding to a stellar mass of $\lesssim 10^8 M_\odot$. Generally speaking, few (S)MBHs are expected to exist in galaxies with a similar stellar mass or lower. Therefore, the EVCC should contain the majority, if not all, of member galaxies within which an X-ray AGN could be present.

The FCC, on the other hand, is a photography-based catalog containing 340 likely members in a footprint of $6^\circ \times 6^\circ$ (2.0 Mpc \times 2.0 Mpc; at the nominal distance of 20.0 Mpc of Fornax; Blakeslee et al. 2009), reaching out to ~ 1.5 times the virial radius ($R_{200} \approx 0.7$ Mpc; Drinkwater et al. 2001). The FCC has a completeness limit of $B_T \sim 18$ mag (an absolute magnitude of $M_{B_T} \sim -13.5$), which corresponds to a stellar mass $\sim 10^8 M_\odot$. This means that the FCC should also include all member galaxies likely to host an AGN, with the caveat that the membership of most galaxies was not on a spectroscopic basis.

3. IDENTIFICATION OF NUCLEAR X-RAY SOURCES

To identify a putative X-ray AGN, we cross-match the galactic nuclei, whose sky coordinates are provided by the EVCC and FCC, with the newly released all-sky survey X-ray source catalogs from eRASS1 (Merloni et al. 2024), which include a soft-band (0.2–2.3 keV) cat-

alog and a hard-band (2.3–5 keV) catalog. We adopt a matching radius of $10''$, corresponding to the 99 percentile of the position error of the soft-band sources, which spans a linear scale of ~ 0.8 (~ 1.0 kpc) at the distance of Virgo (Fornax).

For Virgo, we find a total of 50 point-like X-ray sources positionally coincident with the optical nuclei (Figure 1). Among them, 49 are from the soft band, with 0.2–2.3 keV luminosities ($L_{0.2-2.3}$) ranging between $9.2 \times 10^{38} \text{ erg s}^{-1} - 3.1 \times 10^{41} \text{ erg s}^{-1}$. We take the peak of the 0.2–2.3 keV flux distribution of all eRASS1 sources detected within the EVCC footprint as a rough indicator of the detection completeness limit, which corresponds to $\sim 1.6 \times 10^{39} \text{ erg s}^{-1}$ at the distance of Virgo (Figure 2). This value is also roughly consistent with the aperture photometry based sensitivity map provided by eRASS1, which suggests a 50% completeness limit of $\sim 6.6 \times 10^{-14} \text{ erg s}^{-1} \text{ cm}^{-2}$ ($\sim 2.2 \times 10^{39} \text{ erg s}^{-1}$). Three sources (EVCC 270, 576, 965) are detected in the hard band, among which one source (EVCC 576 = NGC 4388) is detected in the hard band only. The 2.3–5 keV luminosity of these sources is 6.0×10^{41} , 9.2×10^{40} and $2.3 \times 10^{41} \text{ erg s}^{-1}$, respectively.

We estimate the number of potential random matches by artificially shifting the centroid of all X-ray sources within the EVCC footprint by $\pm 3'$ in either *R.A.* or *Decl.*, an amount sufficiently large compared to the default matching radius but also sufficiently small compared to the angular range of the member galaxies. This exercise results in a random match of 1.0 sources aver-

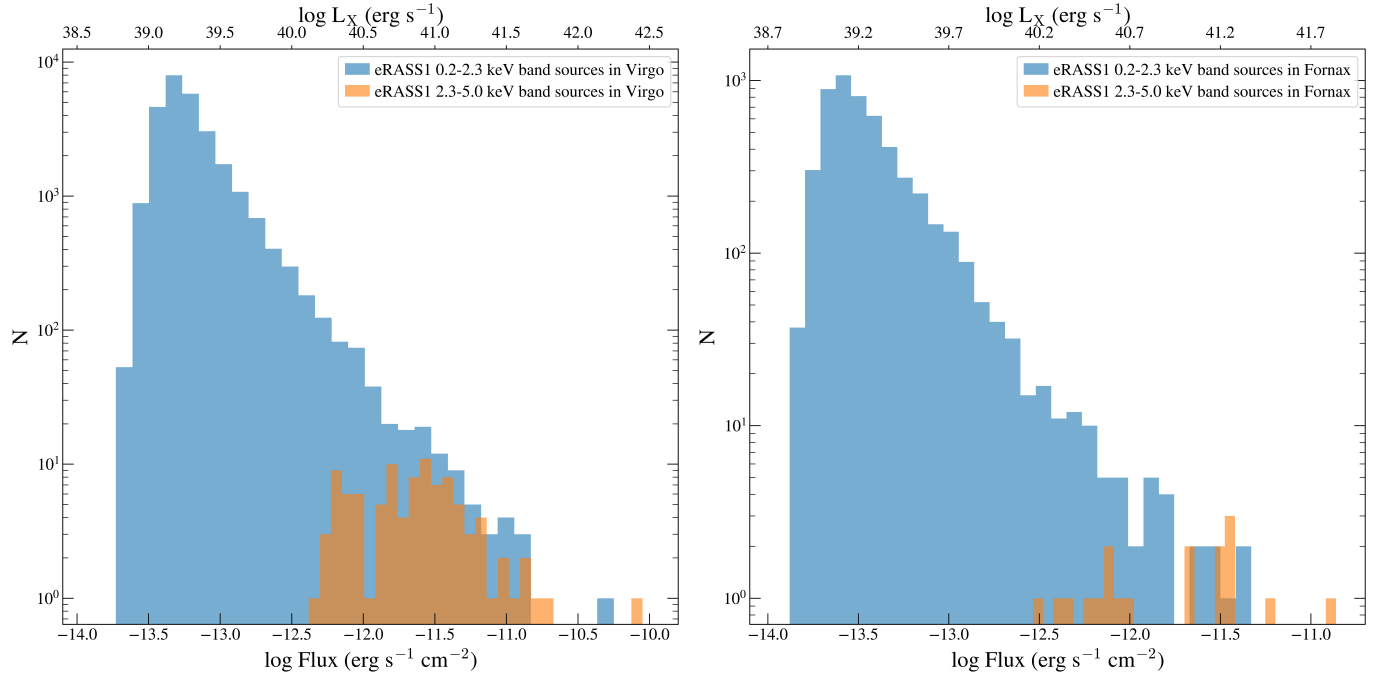


Figure 2. X-ray flux and luminosity distributions of all the eRASS1 point sources in the Virgo (*left*) and Fornax (*right*) footprint. Soft band and hard band sources are shown in blue and orange histograms. The peak of the distributions indicates the detection completeness limit.

aged over the four directions, which may account for only 2% of the actual matches.

In the case of Fornax, originally 11 nuclear X-ray sources were found. After consulting with the NASA/IPAC Extragalactic Database (NED)¹, we find that one galaxy (FCC 129) has a large redshift that disputes its Fornax membership, while the other 10 galaxies have a redshift compatible with Fornax. Therefore, we retain a total of 10 nuclear sources (Figure 1), which are all detected in the soft band, with $L_{0.2-2.3}$ ranging between $9.6 \times 10^{38} \text{ erg s}^{-1}$ – $2.1 \times 10^{41} \text{ erg s}^{-1}$. We note that the eRASS1 source detection completeness limit is $\sim 1.2 \times 10^{39} \text{ erg s}^{-1}$ within the footprint of FCC (Figure 2). Only one galaxy (FCC 121 = NGC 1365) is detected in the hard band with a 2.3–5 keV luminosity of $6.6 \times 10^{41} \text{ erg s}^{-1}$. We find 0.5 random matches for the Fornax galaxies.

Table 1 lists the host galaxy name, centroid coordinates, X-ray luminosity of the matched eRASS1 source, and stellar mass. The stellar mass of the Virgo galaxies is calculated based on the SDSS *g*- and *r*-band photometry given by the EVCC and the color-magnitude relation of Bell et al. (2003). Since only a single band photometry is provided by the FCC, we instead employ the WISE (Wright et al. 2010) W1 and W2 band images to calcu-

late the stellar mass, following the calibration of Jarrett et al. (2019). We have adopted the nominal distances of Virgo and Fornax when deriving the X-ray luminosity and stellar mass.

Comparison with Gallo et al. (2010). The AMUSE-Virgo program detected 32 nuclear X-ray sources out of 100 ETGs in Virgo down to a limiting luminosity of $3.7 \times 10^{38} \text{ erg s}^{-1}$ over 0.5–7 keV (corresponds to $3.2 \times 10^{38} \text{ erg s}^{-1}$ in the 0.2–2.3 keV by assuming an absorbed power-law model with the photon index of 2 and column density $N_{\text{H}} = 2.5 \times 10^{20} \text{ cm}^{-2}$ adopted in Gallo et al. 2010). We find 3 eRASS1 detections among these 32 targets (EVCC 353, 681, 2211), while among the 68 non-detected ETGs, two (EVCC 626, 884) have an eRASS1 match. The non-detection of the remaining targets can be mainly attributed to a lack of sensitivity, because most of them had an X-ray luminosity below $10^{39} \text{ erg s}^{-1}$ according to Gallo et al. (2010). Particularly worth mentioning is M 87, the nuclear source of which has an X-ray luminosity $\sim 10^{41} \text{ erg s}^{-1}$ but is still undetected by eRASS1. This is likely due to the heavy contamination by the surrounding diffuse hot gas in this brightest cluster galaxy.

Comparison with Soria et al. (2022). Soria et al. (2022) reported that a total of 39 nuclear X-ray sources are present among the 75 LTGs in Virgo with a typical detection limit of $\sim 3 \times 10^{38} \text{ erg s}^{-1}$ and a completeness limit of $\sim 10^{39} \text{ erg s}^{-1}$ in the 0.3–10 keV band, but with-

¹ <https://ned.ipac.caltech.edu>

out quoting the exact host galaxies. As a byproduct of our recent study of diffuse hot gas in these LTGs (Hou et al. 2024), we have independently detected 35 nuclear X-ray sources. Among them, 13 share the same host galaxy as the eRASS1 nuclear sources. One additional galaxy, EVCC 595, has an eRASS1 detection.

Comparison with Lee et al. (2019). Lee et al. (2019) detected a total of 11 out of 29 ETGs in Fornax down to a limiting luminosity of $5 \times 10^{38} \text{ erg s}^{-1}$ over 0.3–10 keV, all having an X-ray luminosity below $\sim 2 \times 10^{39} \text{ erg s}^{-1}$. We find only one eRASS1 match (with FCC 153) among these 11 targets and one additional eRASS1 match (with FCC 147) among the 18 non-detected galaxies.

Table 1. Nuclear X-ray sources and host galaxy properties

Name	NGC	RA	DEC	Morph.	$\log L_X$	$\log M_*$
		(deg)	(deg)		(erg s^{-1})	(M_\odot)
(1)	(2)	(3)	(4)	(5)	(6)	(7)
EVCC	(Virgo)					
86	–	180.7616	6.5014	Irr	$39.58^{+0.13}_{-0.14}$	7.9
93	4064	181.0469	18.4442	SB0	$39.47^{+0.15}_{-0.18}$	10.2
107	4123	182.0464	2.8786	SBc	$39.30^{+0.19}_{-0.22}$	10.1
153	4162	182.9690	24.1233	Sc	$39.33^{+0.19}_{-0.22}$	9.8
176	4180	183.2627	7.0389	Sb	$39.23^{+0.20}_{-0.25}$	9.9
241	–	184.0418	15.1236	dE	$39.14^{+0.20}_{-0.26}$	7.8
251	4224	184.1408	7.4619	Sa	$39.60^{+0.20}_{-0.09}$	10.3
267	4233	184.2820	7.6243	SB0	$39.34^{+0.18}_{-0.19}$	10.2
270	4235	184.2912	7.1915	Sa	$41.50^{+0.01}_{-0.02}$	10.3
349	–	184.8695	17.2305	dS0	$39.13^{+0.21}_{-0.25}$	9.0
353	4267	184.9386	12.7982	SB0	$39.38^{+0.16}_{-0.18}$	10.6
355	4268	184.9467	5.2837	Sa	$39.33^{+0.14}_{-0.16}$	9.8
357	–	184.9713	1.7733	Irr	$39.09^{+0.21}_{-0.25}$	8.2
359	4273	184.9833	5.3424	SBc	$39.45^{+0.12}_{-0.13}$	9.8
399	–	185.2976	17.6387	Irr	$39.22^{+0.19}_{-0.21}$	8.6
489	4342	185.9125	7.0540	S0	$39.65^{+0.10}_{-0.11}$	10.1
555	4383	186.3561	16.4699	S0	$39.73^{+0.12}_{-0.12}$	9.8
576*	4388	186.4442	12.6629	Sa	$\lesssim 39.7$	10.4
595	4402	186.5306	13.1125	Sb	$39.46^{+0.16}_{-0.18}$	10.2
626	4417	186.7103	9.5844	S0	$39.34^{+0.13}_{-0.15}$	10.5
634	4419	186.7348	15.0476	Sa	$39.52^{+0.14}_{-0.16}$	10.5
637	4421	186.7606	15.4616	SB0	$39.26^{+0.19}_{-0.20}$	10.2
673	4438	186.9381	13.0110	Sb	$40.01^{+0.09}_{-0.09}$	10.8
681	4442	187.0162	9.8037	SB0	$39.19^{+0.16}_{-0.19}$	10.8
884	4526	188.5127	7.6993	S0	$39.74^{+0.10}_{-0.11}$	11.2
886	4527	188.5357	2.6529	Sb	$39.37^{+0.16}_{-0.19}$	10.8
889	4531	188.5662	13.0754	Sa	$39.15^{+0.17}_{-0.20}$	10.2
892	4535	188.5844	8.1982	SBc	$39.44^{+0.15}_{-0.17}$	10.6
930	4561	189.0339	19.3227	SBd	$39.88^{+0.09}_{-0.10}$	9.3
938	4568	189.1431	11.2394	Sc	$39.58^{+0.13}_{-0.14}$	10.5
965	4579	189.4310	11.8182	SBb	$41.20^{+0.02}_{-0.02}$	11.1
1006	–	189.9501	12.9739	S0	$39.18^{+0.18}_{-0.22}$	9.2
1080	4639	190.7185	13.2571	SBb	$40.11^{+0.07}_{-0.07}$	9.9

Table 1 continued

Table 1 (continued)

Name	NGC	RA	DEC	Morph.	$\log L_X$	$\log M_*$
		(deg)	(deg)		(erg s^{-1})	(M_\odot)
(1)	(2)	(3)	(4)	(5)	(6)	(7)
1102	4651	190.9280	16.3938	Sc	$39.77^{+0.10}_{-0.10}$	10.4
1170	4691	192.0565	-3.3323	SBa	$39.75^{+0.09}_{-0.11}$	10.3
1171	4694	192.0628	10.9835	S0	$39.30^{+0.30}_{-0.11}$	10.1
1182	4710	192.4126	15.1657	S0	$39.35^{+0.17}_{-0.18}$	10.6
1202	4746	192.9801	12.0830	Sc	$39.46^{+0.14}_{-0.16}$	9.7
1216	4765	193.3105	4.4634	Sm	$39.56^{+0.12}_{-0.14}$	9.2
1237	4809	193.7128	2.6525	Irr	$39.18^{+0.18}_{-0.23}$	8.7
2034	4179	183.2171	1.2997	S0	$38.96^{+0.21}_{-0.24}$	10.5
2111	4429	186.8607	11.1077	S0	$39.32^{+0.15}_{-0.18}$	10.9
2124	4450	187.1218	17.0846	Sb	$40.13^{+0.06}_{-0.07}$	10.9
2129	4457	187.2459	3.5706	Sa	$39.90^{+0.08}_{-0.09}$	10.6
2154	4503	188.0260	11.1764	Sa	$39.15^{+0.20}_{-0.23}$	10.5
2169	4536	188.6130	2.1878	Sc	$39.48^{+0.13}_{-0.16}$	10.5
2174	4548	188.8610	14.4955	SBb	$39.25^{+0.14}_{-0.16}$	10.8
2211	4638	190.6976	11.4425	S0	$39.42^{+0.15}_{-0.18}$	10.4
2240	4772	193.3713	2.1684	Sa	$39.66^{+0.11}_{-0.11}$	10.4
2254	4866	194.8628	14.1712	Sa	$39.26^{+0.17}_{-0.19}$	10.5
FCC	(Fornax)					
22	1317	50.68521	-37.10322	Sa	$39.72^{+0.09}_{-0.10}$	10.6
29	1326	50.98410	-36.46461	SBa	$39.65^{+0.09}_{-0.10}$	10.7
57	–	51.86572	-35.92211	dE6	$38.98^{+0.19}_{-0.23}$	7.7
62	1341	51.99234	-37.14789	Sbc	$39.32^{+0.13}_{-0.15}$	9.6
88	1350	52.78314	-33.62839	SBb	$39.53^{+0.10}_{-0.12}$	10.9
121	1365	53.40071	-36.13970	SBbc	$41.31^{+0.01}_{-0.01}$	10.6
147	1374	53.81984	-35.22605	E0	$39.22^{+0.16}_{-0.20}$	10.6
153	–	53.87885	-34.44572	S0	$39.22^{+0.15}_{-0.17}$	10.2
179	1386	54.19280	-35.99919	Sa	$40.23^{+0.04}_{-0.05}$	9.6
222	–	54.80533	-35.36965	dE0	$39.28^{+0.16}_{-0.20}$	8.6

Note—(1) Galaxy Name as in the EVCC and FCC catalogs. (2) NGC name of the galaxy. (3)–(4) Right ascension and declination at equinox J2000 of the galactic nuclei. (5) The morphological type of the galaxy. (6) X-ray luminosity and 1σ error in the 0.2–2.3 keV energy band. *Non-detected. (7) Stellar mass of the galaxy. For Virgo galaxies, this is derived from the $g-r$ mass-luminosity relation, with a typical uncertainty of ~ 0.1 dex. For Fornax galaxies, this is derived from WISE W1- and W2-band images, with a typical uncertainty of $\sim 0.1 - 0.2$ dex. FCC 222 has a larger uncertainty of 1 dex due to its low luminosity. FCC 57 is too faint to be reliably measured in the WISE images, hence its stellar mass a rough estimate from its B_T mag.

4. STATISTICAL PROPERTIES

4.1. Potential contamination by host galaxy

Due to the moderate resolution of eROSITA, the detected nuclear X-ray sources might be contaminated by non-nuclear X-ray emission of the host galaxy. In particular, low mass X-ray binaries (LMXBs), the amount and total X-ray luminosity of which scale with the stellar mass, is expected to produce a 0.2–2.3 keV luminosity of $L_{\text{LMXB}} \approx 7.9 \times 10^{38} \text{ erg s}^{-1} (M_*/10^{10} M_\odot)$, where M_* is

the stellar mass enclosed within the eRASS1 photometry aperture ($\sim 30''$). The above scaling relation is derived from the empirical $L(2\text{--}10\text{ keV})\text{--}M_*$ relation of [Lehmer et al. \(2010\)](#), and we have assumed for LMXBs an intrinsic power-law spectrum with a canonical photon-index of 1.7. Based on the EVCC, we find that the majority of matched galaxies have an optical size (r_{Kron}) above $30''$ (i.e., well resolved by eROSITA); only a few galaxies having the lowest stellar masses ($\lesssim 10^9 M_\odot$) are entirely covered by the eRASS1 source aperture. Therefore, we conclude that statistically LMXBs have only a small contribution to the detected nuclear X-ray emission.

A small fraction of the matched galaxies could be actively forming stars, which would also contribute to the observed X-ray emission in the form of high-mass X-ray binaries and/or diffuse hot gas. The 0.2–2.3 keV luminosity of this star formation-related component is estimated as ([Lehmer et al. 2016](#)): $L_{\text{SF}} \approx 5.6 \times 10^{39} \text{ erg s}^{-1} (\text{SFR}/M_\odot \text{ yr}^{-1})$, for which a factor of 1.4 is multiplied to the original scaling relation to roughly account for a different photon energy range (0.5–2 keV). Since no explicit information about the star formation rate (SFR) is provided by the EVCC, we employ the WISE W3-band image to estimate the SFR, following [Jarrett et al. \(2019\)](#). We find that all but two of the 50 host galaxies in Virgo have an SFR within the eRASS1 source aperture too low to have a significant contribution to the observed nuclear X-ray emission. The two exceptions are EVCC 359 and EVCC 892 which have a central SFR $\sim 1.7 M_\odot \text{ yr}^{-1}$ and $\sim 0.4 M_\odot \text{ yr}^{-1}$, sufficient to explain the observed nuclear X-ray emission. Therefore, we conclude that statistically star-forming activities also have only a minor contribution to the detected nuclear X-ray emission.

By evaluating the stellar mass and SFR of the 10 Fornax host galaxies, we find that host galaxy contamination can be neglected in all but three galaxies. FCC 22, FCC 29 and FCC 62 have a substantial SFR to account for the observed X-ray emission. Moreover, it is still possible that a small fraction of the eRASS1 nuclear sources are X-ray binaries rather than a genuine AGN, because the detection limit of eRASS1 is still compatible with the Eddington limit of stellar-mass black holes. We note that the same caveat holds for the aforementioned *Chandra* programs, which all have an even lower detection limit.

4.2. Host galaxies and occupation fraction

Following the convention, we collectively assign ellipticals, lenticulars and dwarf ellipticals/lenticulars as ETGs, and the remaining morphological types as LTGs.

For Virgo, when the EVCC morphological type is ‘edge-on’, we consult with NED to determine the morphological type if available; for those without an explicit morphological type, we take them as ETGs, introducing only a $\sim 2.5\%$ ambiguity. The ETG fraction of Virgo is thus $\sim 49\%$. A much higher fraction of $\sim 82\%$ is found in Fornax according to the FCC, with the caveat that the FCC classification was based on old imaging data probably less sensitive than SDSS. It turns out that 17 of the 50 Virgo hosts are ETGs, while 4 of the 10 Fornax hosts are ETGs, indicating a similar percentage ($34\% \pm 10\%$ vs. $40\% \pm 24\%$) in the two clusters. Quoted errors are of Poisson and at 1σ confidence level.

The percentage of X-ray detected nuclei, or the *occupation rate* of an X-ray AGN, is also quite similar between Virgo and Fornax ($50/1589 \approx 3.1\% \pm 0.4\%$ vs. $10/340 \approx 2.9\% \pm 0.9\%$). The occupation rate becomes $\approx 2.6\% \pm 0.4\%$ and $\approx 2.6\% \pm 0.9\%$, if we drop 9 sources in Virgo and 1 source in Fornax, whose X-ray luminosities are below the detection completeness limit (Section 3). If instead we restrict on host galaxies with $\log(M_*/M_\odot) > 7.8$, which is the lowest mass among the 50 Virgo hosts and also is roughly the completeness limit of the EVCC, the percentage becomes $4.2 \pm 0.6\%$ ($50/1203$).

We further evaluate the occupation rate by dividing the Virgo galaxies into subgroups, according to the stellar mass, the projected distance from the center of M 87, and the morphological type (ETG or LTG), respectively. Due to the small number of X-ray nuclei in Fornax, we do not perform a similar analysis.

As expected, while the majority of EVCC galaxies are actually dwarfs, only four X-ray nuclei are detected among galaxies with $7.8 < \log(M_*/M_\odot) < 8.65$ ($4/602 \approx 0.7 \pm 0.3\%$), compared to 46 in the more massive group ($46/601 \approx 7.7 \pm 1.1\%$). On the other hand, a comparable occupation rate ($3.6 \pm 0.7\%$ vs. $2.6 \pm 0.6\%$) is found between galaxies located inside and outside $\sim 1.7R_{200}$ of Virgo. Intuitively, those galaxies on the first infall to the cluster core may still contain a significant amount of ISM to fuel the central SMBH, but this effect could be offset by the on-average heavier SMBHs in galaxies already in or passing the cluster core due to frequent galaxy merger therein. A full spectroscopic survey of the nuclei of the EVCC galaxies would be desired to provide a robust and uniform measurement of black hole mass and hence the Eddington ratio. Finally, a marginally significant ($\sim 2\sigma$) difference in the occupation rate is seen between the ETGs and LTGs ($2.2 \pm 0.5\%$ vs. $4.0 \pm 0.7\%$). This is consistent with the naive expectation that LTGs contain more available fuel for the SMBH.

5. SUMMARY AND DISCUSSION

In this work, we have utilized the newly released X-ray source catalogs from the first all-sky scan of eROSITA to probe putative X-ray AGNs in the Virgo and Fornax clusters, taking advantage of its full coverage of all known member galaxies.

A total of 50 and 10 X-ray sources are found to be positionally coincident with the nuclei of member galaxies in Virgo and Fornax, respectively. A large fraction of these nuclear X-ray sources are identified for the first time. Despite the moderate resolution of eROSITA, we find that in most cases host galaxy contamination is negligible to the observed X-ray luminosity, indicating the dominance of a genuine X-ray AGN. The majority of these nuclear X-ray sources are found in late-type hosts.

The overall occupation rate of the eRASS1 nuclear sources is remarkably low, $\sim 3\%$ in both clusters. This appears to be much lower than found in nearby galaxies not residing in clusters. For instance, at least 13% of the AMUSE-Field ETGs have an X-ray luminosity $\gtrsim 2 \times 10^{39} \text{ erg s}^{-1}$ (Miller et al. 2012), i.e., above the eRASS1 completeness limit. In a *Chandra* survey of X-ray AGNs in 719 galaxies within a distance of 50 Mpc (most are outside Virgo and Fornax), She et al. (2017) found 314 X-ray nuclei, among which $\sim 50\%$ have an X-ray luminosity above the eRASS1 completeness limit. Although not free of selection effect, these two studies imply that the occupation rate of an X-ray AGN in field galaxies is likely higher than 10%. Hence, the relatively low occupation rate in Virgo and Fornax strongly suggests that AGN activity is generally suppressed in the cluster environment.

A related and equally remarkable feature about the eRASS1 nuclear X-ray sources is the paucity of luminous objects. Indeed the highest 0.2–2.3 keV luminosity found is only $\sim 3 \times 10^{41} \text{ erg s}^{-1}$, which would correspond to $\sim 1\%$ Eddington even for a black hole mass as low as $10^5 M_{\odot}$. For comparison, the maximum luminosity of the X-ray nuclei detected by She et al. (2017) well exceeds this value, regardless of the host galaxy morphological type. A potential issue here is that the Virgo and Fornax nuclear X-ray sources are essentially detected in soft X-rays, which might be subject to circumnuclear absorption. However, it is unlikely that a large number of obscured AGNs are present in present-day clusters, in which gas-rich galaxies are not a significant population. The few detections of nuclear sources in the eRASS1 2.3–5 keV catalog supports this notion. Alternatively,

as found by Birchall et al. (2020, 2022), the steep X-ray AGN luminosity function naturally implies a rarity of luminous objects in volume-limited samples. Regardless, the first complete census of AGNs in Virgo and Fornax in the soft X-rays would provide useful constraints for cosmological simulations of galaxy cluster formation (Nelson et al. 2023).

A small but non-negligible fraction of the eRASS1 nuclear X-ray sources are associated with dwarf galaxies, which may host a dwarf MBH. High-resolution *Chandra* observations are desired to determine whether these sources are genuine AGNs. Moreover, some of the eRASS1 nuclear X-ray sources have been previously detected or undetected by *Chandra* observations (Section 3). The subsequent scans of eROSITA would shed light on the flux variability of these sources.

M.H. is supported by the National Natural Science Foundation of China (grant 12203001) and the fellowship of China National Postdoctoral Program for Innovation Talents (grant BX2021016). Z.H. and Z.L. acknowledge the support of the National Natural Science Foundation of China (grant 12225302) and the National Key Research and Development Program of China (NO.2022YFF0503402). The authors wish to thank Lin He for help with the eRASS1 data.

This work is based on data from eROSITA, the soft X-ray instrument aboard SRG, a joint Russian-German science mission supported by the Russian Space Agency (Roskosmos), in the interests of the Russian Academy of Sciences represented by its Space Research Institute (IKI), and the Deutsches Zentrum für Luftund Raumfahrt (DLR). The SRG spacecraft was built by Lavochkin Association (NPOL) and its subcontractors, and is operated by NPOL with support from the Max Planck Institute for Extraterrestrial Physics (MPE). The development and construction of the eROSITA X-ray instrument was led by MPE, with contributions from the Dr. Karl Remeis Observatory Bamberg & ECAP (FAU Erlangen-Nuernberg), the University of Hamburg Observatory, the Leibniz Institute for Astrophysics Potsdam (AIP), and the Institute for Astronomy and Astrophysics of the University of Tübingen, with the support of DLR and the Max Planck Society. The Argelander Institute for Astronomy of the University of Bonn and the Ludwig Maximilians Universität Munich also participated in the science preparation for eROSITA.

REFERENCES

- Bell, E. F., McIntosh, D. H., Katz, N., & Weinberg, M. D. 2003, *ApJS*, 149, 289, doi: [10.1086/378847](https://doi.org/10.1086/378847)
- Binggeli, B., Sandage, A., & Tammann, G. A. 1985, *AJ*, 90, 1681, doi: [10.1086/113874](https://doi.org/10.1086/113874)

- Birchall, K. L., Watson, M. G., & Aird, J. 2020, *MNRAS*, 492, 2268, doi: [10.1093/mnras/staa040](https://doi.org/10.1093/mnras/staa040)
- Birchall, K. L., Watson, M. G., Aird, J., & Starling, R. L. C. 2022, *MNRAS*, 510, 4556, doi: [10.1093/mnras/stab3573](https://doi.org/10.1093/mnras/stab3573)
- Blakeslee, J. P., Jordán, A., Mei, S., et al. 2009, *ApJ*, 694, 556, doi: [10.1088/0004-637X/694/1/556](https://doi.org/10.1088/0004-637X/694/1/556)
- Boselli, A., Fossati, M., & Sun, M. 2022, *A&A Rv*, 30, 3, doi: [10.1007/s00159-022-00140-3](https://doi.org/10.1007/s00159-022-00140-3)
- Drinkwater, M. J., Gregg, M. D., Holman, B. A., & Brown, M. J. I. 2001, *MNRAS*, 326, 1076, doi: [10.1046/j.1365-8711.2001.04646.x](https://doi.org/10.1046/j.1365-8711.2001.04646.x)
- Fabian, A. C. 2012, *ARA&A*, 50, 455, doi: [10.1146/annurev-astro-081811-125521](https://doi.org/10.1146/annurev-astro-081811-125521)
- Ferguson, H. C. 1989, *AJ*, 98, 367, doi: [10.1086/115152](https://doi.org/10.1086/115152)
- Gallo, E., Treu, T., Jacob, J., et al. 2008, *ApJ*, 680, 154, doi: [10.1086/588012](https://doi.org/10.1086/588012)
- Gallo, E., Treu, T., Marshall, P. J., et al. 2010, *ApJ*, 714, 25, doi: [10.1088/0004-637X/714/1/25](https://doi.org/10.1088/0004-637X/714/1/25)
- Giacconi, R., Zirm, A., Wang, J., et al. 2002, *ApJS*, 139, 369, doi: [10.1086/338927](https://doi.org/10.1086/338927)
- Goulding, A. D., Greene, J. E., Setton, D. J., et al. 2023, *ApJL*, 955, L24, doi: [10.3847/2041-8213/acf7c5](https://doi.org/10.3847/2041-8213/acf7c5)
- Graham, A. W., Soria, R., Davis, B. L., et al. 2021, *ApJ*, 923, 246, doi: [10.3847/1538-4357/ac34f4](https://doi.org/10.3847/1538-4357/ac34f4)
- Greene, J. E., Strader, J., & Ho, L. C. 2020, *ARA&A*, 58, 257, doi: [10.1146/annurev-astro-032620-021835](https://doi.org/10.1146/annurev-astro-032620-021835)
- Ho, L. C. 2008, *ARA&A*, 46, 475, doi: [10.1146/annurev.astro.45.051806.110546](https://doi.org/10.1146/annurev.astro.45.051806.110546)
- Hou, M., He, L., Hu, Z., et al. 2024, *ApJ*, 961, 249, doi: [10.3847/1538-4357/ad138a](https://doi.org/10.3847/1538-4357/ad138a)
- Hu, Z., Su, Y., Li, Z., et al. 2023, *ApJ*, 956, 104, doi: [10.3847/1538-4357/acf292](https://doi.org/10.3847/1538-4357/acf292)
- Jarrett, T. H., Cluver, M. E., Brown, M. J. I., et al. 2019, *ApJS*, 245, 25, doi: [10.3847/1538-4365/ab521a](https://doi.org/10.3847/1538-4365/ab521a)
- Kim, S., Rey, S.-C., Jerjen, H., et al. 2014, *ApJS*, 215, 22, doi: [10.1088/0067-0049/215/2/22](https://doi.org/10.1088/0067-0049/215/2/22)
- Kormendy, J., & Ho, L. C. 2013, *ARA&A*, 51, 511, doi: [10.1146/annurev-astro-082708-101811](https://doi.org/10.1146/annurev-astro-082708-101811)
- Lee, N., Gallo, E., Hodges-Kluck, E., et al. 2019, *ApJ*, 874, 77, doi: [10.3847/1538-4357/ab05cd](https://doi.org/10.3847/1538-4357/ab05cd)
- Lehmer, B. D., Alexander, D. M., Bauer, F. E., et al. 2010, *ApJ*, 724, 559, doi: [10.1088/0004-637X/724/1/559](https://doi.org/10.1088/0004-637X/724/1/559)
- Lehmer, B. D., Basu-Zych, A. R., Mineo, S., et al. 2016, *ApJ*, 825, 7, doi: [10.3847/0004-637X/825/1/7](https://doi.org/10.3847/0004-637X/825/1/7)
- Luo, B., Brandt, W. N., Xue, Y. Q., et al. 2017, *ApJS*, 228, 2, doi: [10.3847/1538-4365/228/1/2](https://doi.org/10.3847/1538-4365/228/1/2)
- Mei, S., Blakeslee, J. P., Côté, P., et al. 2007, *ApJ*, 655, 144, doi: [10.1086/509598](https://doi.org/10.1086/509598)
- Merloni, A., Lamer, G., Liu, T., et al. 2024, *A&A*, 682, A34, doi: [10.1051/0004-6361/202347165](https://doi.org/10.1051/0004-6361/202347165)
- Miller, B., Gallo, E., Treu, T., & Woo, J.-H. 2012, *ApJ*, 747, 57, doi: [10.1088/0004-637X/747/1/57](https://doi.org/10.1088/0004-637X/747/1/57)
- Nelson, D., Pillepich, A., Ayromlou, M., et al. 2023, *arXiv e-prints*, arXiv:2311.06338, doi: [10.48550/arXiv.2311.06338](https://doi.org/10.48550/arXiv.2311.06338)
- Padovani, P., Alexander, D. M., Assef, R. J., et al. 2017, *A&A Rv*, 25, 2, doi: [10.1007/s00159-017-0102-9](https://doi.org/10.1007/s00159-017-0102-9)
- Schmidt, M. 1963, *Nature*, 197, 1040, doi: [10.1038/1971040a0](https://doi.org/10.1038/1971040a0)
- She, R., Ho, L. C., & Feng, H. 2017, *ApJ*, 835, 223, doi: [10.3847/1538-4357/835/2/223](https://doi.org/10.3847/1538-4357/835/2/223)
- Shi, F., Li, Z., Yuan, F., & Zhu, B. 2021, *Nature Astronomy*, 5, 928, doi: [10.1038/s41550-021-01394-0](https://doi.org/10.1038/s41550-021-01394-0)
- Simionescu, A., Werner, N., Mantz, A., Allen, S. W., & Urban, O. 2017, *MNRAS*, 469, 1476, doi: [10.1093/mnras/stx919](https://doi.org/10.1093/mnras/stx919)
- Soria, R., Kolehmainen, M., Graham, A. W., et al. 2022, *MNRAS*, 512, 3284, doi: [10.1093/mnras/stac148](https://doi.org/10.1093/mnras/stac148)
- Sunyaev, R., Arefiev, V., Babyshkin, V., et al. 2021, *A&A*, 656, A132, doi: [10.1051/0004-6361/202141179](https://doi.org/10.1051/0004-6361/202141179)
- Weinberger, R., Springel, V., Hernquist, L., et al. 2017, *MNRAS*, 465, 3291, doi: [10.1093/mnras/stw2944](https://doi.org/10.1093/mnras/stw2944)
- Wright, E. L., Eisenhardt, P. R. M., Mainzer, A. K., et al. 2010, *AJ*, 140, 1868, doi: [10.1088/0004-6256/140/6/1868](https://doi.org/10.1088/0004-6256/140/6/1868)
- Xue, Y. Q. 2017, *NewAR*, 79, 59, doi: [10.1016/j.newar.2017.09.002](https://doi.org/10.1016/j.newar.2017.09.002)
- Yoon, D., Yuan, F., Ostriker, J. P., Ciotti, L., & Zhu, B. 2019, *ApJ*, 885, 16, doi: [10.3847/1538-4357/ab45e8](https://doi.org/10.3847/1538-4357/ab45e8)
- Yuan, F., & Narayan, R. 2014, *ARA&A*, 52, 529, doi: [10.1146/annurev-astro-082812-141003](https://doi.org/10.1146/annurev-astro-082812-141003)